Mass-Energy Compensation Effect of 3α Hamiltonian

I. Filikhin[1], C. Martin[1], A. Karoui[2], and B. Vlahovic[1*]

[1] *CREST/Mathematics and Physics Department,*

North Carolina Central University, Durham, USA

[2] *Elizabeth City State University,*

Elizabeth City, USA

Abstract

The 3α phenomenological model describes the structure of the carbon-12 nucleus as a cluster of three alpha particles. This model includes a pairwise α–α interaction and a three-body force. To fit the three-body potential, the ^{12}C data are used, while ensuring that the pair potential reproduces the α–α scattering data. Alternatively, the mass-energy compensation (MEC) effect can be used to simulate the effect of the three-body potential by adjusting the mass of the α particle within the effective-mass approach. We demonstrate the MEC effect for the 3α ground state by numerically solving the differential Faddeev equation, in which the α–α interaction is described by the Ali-Bodmer potential. The effective masses of α particles are evaluated for the ground and excited 0^+ and bound 2^+ states. We demonstrate a coupling between the ground and first excited 0^+ states, indicated by an anti-crossing of these energy levels in the energy–mass coordinates. A correspondence between the effective mass and a three-body potential is demonstrated. We discuss the results of the 0_2^+ calculations for various models of the α–α interaction.

* ifilikhin@nccu.edu

I. INTRODUCTION

We explore the application of the effective mass concept from solid-state physics [1] and many-body physics [2] to investigate nuclear few-body systems such as $3N$ and 3α. Our approach is rooted in a notable property of a three-body nuclear Hamiltonian for bound states, known as mass-energy compensation (MEC), as described in Refs. [3–5]. The MEC embodies the general physical relationship between mass and energy, notably manifesting itself in the mass defect formula for nuclei. In a recent study [3], we delved into the mass-energy compensation for the three-nucleon Hamiltonian and developed a new phenomenological approach to characterize the three-body force in $3N$ systems. The effective mass of a nucleon is introduced to offset the effects of this proposed three-body force. We extended this approximation to another nuclear system of identical particles - the three alpha particles system, representing the cluster model for the ^{12}C nucleus. In Ref. [5], we defined the effective mass for each low-lying level of this nucleus based on the effective mass approach. This work serves as a continuation of the previous study [5], with a particular focus on the resonance state 0_2^+ in the ^{12}C nucleus.

The α-cluster model for ^{12}C was initially proposed in Ref. [6] due to observed clustering properties in the low-lying states of ^{12}C. As known, the fusion of two α-particles forms the ^{8}Be nucleus. A third α-particle can then fuse with ^{8}Be, resulting in the formation of the ^{12}C nucleus. The fusion of ^{8}Be and an α-particle leads to the creation of a higher-energy resonance state (0_2^+), famously known as the Hoyle state [7]. This resulting 3α system releases excess energy through a gamma-ray burst, transitioning from the excited formation state (0_2^+) to the more stable ground state (0_1^+). The coupling between the Hoyle state (0_2^+) and the ground state (0_1^+) enhances the cross-section for the fusion reaction, facilitating the creation of a stable ^{12}C nucleus before decay. This process is crucial for stellar nucleosynthesis, contributing to the formation of other light elements in stars, which serve as the building blocks for heavier elements.

The 3α-clustering phenomenon has been extensively studied through various approaches [10–34]. Different inter-cluster potentials, often derived from α-α scattering data, have been proposed [8, 9]. Several cluster models, including the three-body force (3bf), have been explored [16, 20, 24, 34], reflecting the duality of forming a cluster nuclear structure from cluster states and mean field states [30]. However, describing the low-lying ^{12}C spectrum in

detail within the cluster model faces challenges related to the three-body potential [13, 24]. Notably, the three-body potential cannot be the same for low-lying levels with different total orbital quantum numbers [14]. Furthermore, it can be assumed that the parameters of a three-body potential depend on energies in rotation bands [38] of the 3α system. Depending on the two-body potential used, the three-body potential can be either repulsive [11, 13, 22] or attractive [16, 27]. For instance, a repulsive 3α potential was introduced in Ref. [23], dependent on the total angular momentum J=0^+, 2^+, and 4^+. The potential has a Gaussian form with depths $V(0^+)$=31.7 MeV, $V(2^+)$=63.0 MeV, and $V(4^+)$=150.0 MeV [24]. In contrast, an attractive three-body potential was proposed in Refs. [10, 14, 16, 26, 39]. In these corresponding 3α-cluster models, the phenomenological pair potential with s, d, and g partial components was utilized from Ref. [8]. In Refs. [32, 33] this model was applied to compute momentum and energy distributions of the three α-particles emerging from the decay of low-lying ^{12}C-resonances. Another notable work [34] used the same model in 3α Faddeev calculations. The Faddeev component was factorized by the function $\xi_0(x)$, describing the two-particle cluster (ground state 0^+ of ^{8}Be), and by the function $f(y)$, characterizing the relative motion of the third particle relative to the pair. This model accurately reproduced the experimental parameters of the 0_2^+ resonance. One can state that the AB+ 3bf model with an attractive three-body potential has been applied in numerous papers for calculations of the ^{12}C nucleus properties (for instance see Refs. [35–37]).

Similar considerations were made in Ref. [40], where α-cluster systems were viewed as dilute multi-α cluster condensed states. A combination of the s-wave α–α potential and a repulsive three-body potential of Gaussian type was used to describe the 0_2^+ resonance of the ^{12}C nucleus. This pairing of pair and three-body potentials resulted in a resonance energy value of 0.98 MeV (above the three-body threshold), as reported in Ref. [40]. Importantly, the α–α potential was fitted to reproduce the experimental resonant energy for the ^{8}Be ground state. Additionally, one can particularly highlight the review [41], which provides a concise summary of most theoretical cluster approaches to the Hoyle state.

Our study builds upon the framework proposed in Refs. [5, 14], assuming three terms in the 3α Hamiltonian: kinetic energy, two-body, and three-body potentials. The two-body potential is chosen to reproduce two-body experimental data, while the three-body potential parameters are determined based on ^{12}C data. The Ali-Bodmer (AB) potential was a suitable choice [14], displaying a simple coordinate dependence with a repulsive core in the s partial

wave to mimic Pauli repulsion between two alpha particles. This potential has shown promise in describing cluster systems such as $\alpha\alpha n$ [42] and $\alpha\alpha\Lambda$ [43]. The set of AB and 3α potentials obtained in Ref. [14] satisfactorily describes the low-lying ^{12}C spectrum, with additional adjustments for the three-body potential to achieve accurate spectrum reproduction. In our present work, we use the model from Ref. [14] to establish a general scheme for defining a three-body potential using the effective mass concept. In this scheme, we adjust the alpha particle's mass to describe 3α states and establish a correspondence with a three-body potential. The mass-energy compensation property of the three-body Hamiltonian facilitates this procedure.

Our general goal is to demonstrate the mass-energy compensation effect for the 3α Hamiltonian, which includes two- and three-body interactions. Specifically, we will show how the additional three-body binding energy arising from three-body interactions can be compensated by variations in the mass of the particles. The chosen 3α model is appropriate for this purpose.

The foundation of our study rests on the application of Faddeev equations in coordinate space [44]. This formalism empowers us to handle the Coulomb potential without resorting to approximations, and it enables the use of coordinate-dependent potentials with a well-defined and easily interpretable physical significance.

II. FORMALISM

A. Mass-Energy Compensation

The α-cluster model for the ^{12}C nucleus describes the nucleus as a bound system of three alpha particles. The three-body Hamiltonian reads

$$H = H_0 + V_{2bf} + V_{3bf}. \tag{1}$$

Here, H_0 is the kinetic operator given by $H_0 = \sum_{i=1,2,3} \frac{\pi_i^2}{2m_0}$, where $\pi_i^2 = -\hbar^2\Delta_i$, $i = 1, 2, 3$. The m_0 represents the mass of a free alpha particle. Additionally, V_{2bf} and V_{3bf} denote two-body and three-body interactions, respectively. The three-body potential V_{3bf} is assumed to act as a perturbation.

Ref. [3] introduces the concept of a particle's effective mass m^* in a three-body system. Specifically, the effective nucleon mass is defined through an averaged nucleon mass cor-

rection, compensating for the attractive effect of a three-body force in $3N$ systems. The feasibility of this correction, as discussed in Ref. [3], arises from the mass-energy compensation effect in the three-body Hamiltonian. To elucidate this effect, consider the Hamiltonian expressed in linear form:

$$H = \beta H_0 + \alpha V_{2bf}, \tag{2}$$

where $\beta, \alpha > 0$. One can change the particle mass and the depth of the potential simultaneously by using parameters α and β.

Averaging the Schrödinger equation over the wave function leads to the algebraic form for matrix elements:

$$E = E(\beta, \alpha) = \beta\langle H_0\rangle + \alpha\langle V_{2bf}\rangle. \tag{3}$$

The matrix elements $\langle H_0\rangle$ and $\alpha\langle V_{2bf}\rangle$ have opposite signs. One can vary the parameters around the point $\alpha = \beta = 1$ such that corresponding energy changes are opposite and can be compensated by each other. Thus, we define the mass-energy compensation effect [3–5].

A comparable compensation can be achieved by incorporating a three-particle force into the Hamiltonian (2) as part of the potential energy. To offset the effects of the three-particle force term, we modify the particle's mass as $m^* = m_0 + \Delta m$. The scale parameter β is linked to the effective mass through the relationship $m^*/m_0 = 1/\beta$.

Considering small variations in the mass $m^*/m_0 = 1 + \Delta m/m_0$, where $\Delta m/m_0 \ll 1$, and following Ref. [46], one can express the kinetic energy operator in terms of the individual momenta of the particles in the center-of-mass frame:

$${H_0}^* = \sum_{i=1,2,3} \frac{\pi_i^2}{2m^*} \approx \sum_{i=1,2,3} \frac{\pi_i^2}{2m_0}(1 - \frac{\Delta m}{m_0}). \tag{4}$$

Here, we use Taylor expansion of the function $1/m^*$ in the small vicinity Δm of the value m, taking the first two terms of the expansion. Thus, the corresponding variations for the left-hand side of Eq. (2) can be written as

$$\Delta\langle H_0\rangle \approx -\frac{\langle H_0\rangle}{m_0}\Delta m. \tag{5}$$

This dependence is exactly linear locally near the point $m^*/m_0 = 1$ for the simple case of the s-wave approach for three-nucleon systems, as shown in Ref. [4], and for the more complex case of three-nucleon systems interacting with the AV14 nucleon-nucleon potential, as considered in Ref. [3].

Taking into account a three-particle potential, one can consider the linear form

$$H = \beta H_0 + \alpha V_{2bf} + \gamma V_{3bf}. \tag{6}$$

Here, the three-particle potential is a perturbation. In accordance with the effective mass approach, the Hamiltonian (6), where $\alpha = \gamma = 1$, can be approximated as $H = \beta' H_0 + V_{2bf}$, where β' is greater or less than β depending on the sign of the contribution $\langle V_{3bf} \rangle$ of the three-body potential that we are trying to compensate.

We can infer that the slope of the energy-mass dependence, represented as $E = E(m^*) = \beta \langle H_0 \rangle + \langle V_{2bf} \rangle$, is determined by the attraction or repulsion of this potential. Utilizing the linear form (6), the average kinetic energy can be computed as $\langle H_0 \rangle = \partial E / \partial \beta$, where E denotes the binding energy for the 3α system. The average contribution from the two-body (three-body) potential can be calculated as $\langle V_{2bf} \rangle = \partial E / \partial \alpha|_{\alpha=1}$ ($\langle V3bf \rangle = \partial E / \partial \gamma|_{\gamma=1}$). These equations will be subsequently employed in the numerical evaluation of matrix elements of the Hamiltonian (1).

B. The differential Faddeev Equation

The bound states of the three-particle system are characterized by the Hamiltonian (1). Alternatively, one can describe the system using the differential Faddeev equations for the components of the wave function [44]. In the case of identical particles, the set of Faddeev equations is represented by a single equation of the form [34]:

$$(H_0 + V_{\alpha\alpha} + V_{Coul.} + V_{3bf} - E)U = -V_{\alpha\alpha}(P_c^+ + P_c^-)U, \tag{7}$$

Here, $V_{\alpha\alpha}$ signifies a short-range $\alpha\alpha$ nuclear potential, $V_{Coul.}$ represents the Coulomb force, $H_0 = -\frac{\hbar^2}{m_0}(\Delta_{\mathbf{x}} + \frac{3}{4}\Delta_{\mathbf{y}})$ is the kinetic energy operator and ($\mathbf{x}$, $\mathbf{y}$) are the Jacobi coordinates. The wave function is expressed in terms of the Faddeev component U as follows: $\Psi = (I + P_c^+ + P_c^-)U$, where P_c^+ and P_c^- are cyclic permutation operators of particles. A three-body potential, considered as a perturbation, can be added to the left-hand side of equation (7). The eigenvalue problem for Eq. (7) is numerically solved, with boundary conditions specified for the component U by exponentially decreasing asymptotics.

C. Potentials

Within the α-cluster model for the ^{12}C nucleus, alpha particles interact via pair and three-body nuclear potentials as well as the Coulomb force. We will employ the potentials proposed in Ref. [14]. The phenomenological Ali-Bodmer (AB) α-α potential [8] defines different s, d, and g partial components, written as two-range Gaussians:

$$V_{2bf}(x) = V_1 \exp(-\frac{x^2}{b_1^2}) + V_2 \exp(-\frac{x^2}{b_2^2}), \tag{8}$$

where the strength and range parameters are $V_1 = 500$ MeV, $b_1 = 1.43$fm, $V_2 = -130$ MeV, $b_2 = 2.11$fm for s-wave; $V_1 = 320$ MeV, $b_1 = 1.43$fm, $V_2 = -130$ MeV, $b_2 = 2.11$ fm for d-wave; $V_1 = 0$, $V_2 = -130$ MeV, $b_2 = 2.11$ fm for g-wave. The attractive s-wave component of the potential simulates Pauli blocking. This model can be supplemented with an attractive three-particle potential $V_3(\rho)$ in the form of a single-range Gaussian [14]:

$$V_{3bf}(\rho) = V \exp(-\frac{1}{2}(\frac{\rho}{b})^2), \tag{9}$$

where $\frac{1}{2}\rho^2 = \sum_{i=1}^{i=3} \mathbf{r}_i^2$ and $\mathbf{r_i}$ is the position vector of the i-th α particle relative to the center of mass of the system. This potential does not affect a two-body threshold of a three-body system and was used in Ref. [14] for calculating the bound and resonance states in the 3α system.

A three-body potential acting at short distances can describe the well-known violation of the cluster structure [45]. In line with the concept of effective mass, the contribution from the three-body potential can be compensated by adjusting the mass of the α-particles. This compensation is achieved when the calculated energy matches the experimental value. Depending on the energy level, the effective mass m^* can be less or greater than the free mass m_0. There exists a correlation between the depth (attraction/repulsion) of the three-body potential and the value of the effective mass [5].

III. NUMERICAL RESULTS

Our approach to the ^{12}C nucleus is fundamentally grounded in mass-energy compensation (3). According to Eq. (2), the ground state energy E of the 3α system is expressed as a function of two scaling parameters, α and β, such that $E = E(\beta, \alpha)$. To illustrate the effect of mass and energy compensation, we carried out calculations for two functions: $E(\beta, \alpha =$

1) and $E(\beta = 1, \alpha)$. In these calculations, we neglected the three-particle potential and employed the Ali-Bodmer potential (8) for pair interactions. The numerical results are presented in Fig. 1. The resulting functions exhibit nonlinearity and intersect at the point $\beta = \alpha = 1$. By independently varying the parameters β and α, we are able to replicate the experimental energy of the ^{12}C ground state. This suggests that a change in mass can effectively compensate for any small alteration in the potential energy term.

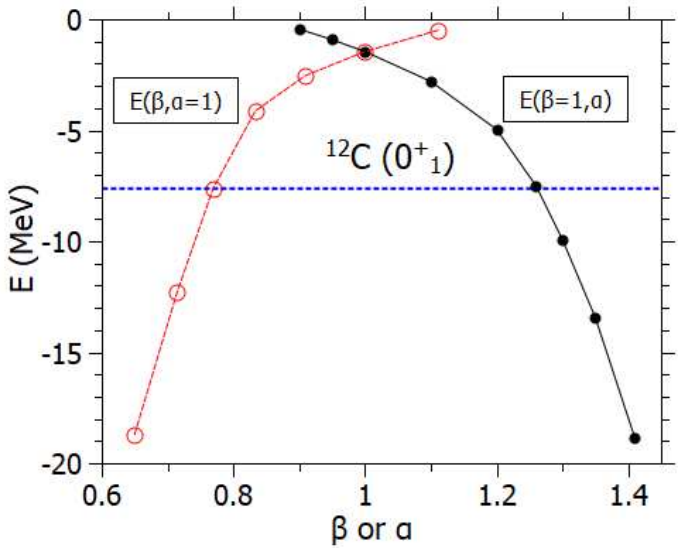

FIG. 1. The $3\alpha(0_1^+)$ ground state energy E as a function of the scaling parameter α or β in Eq. (2) using the Ali-Bodmer potential (8). The dashed line indicates the experimental ground state energy of ^{12}C.

The nonlinear behavior of the function $E(\beta, \alpha = 1)$ as the parameter β decreases is associated with the significant contribution of the three-particle potential, which must be compensated for by an increase in the effective mass. To gauge the impact of variations in the effective mass m^*, one should consider the next term of the Taylor expansion instead of the linear representation in Eq. (4). In this way, the first k terms of the Taylor series for the function $1/m$ must be taken into account near the point $m^*/m_0 = 1$. The energy can be written as $E(m^*) = E(m^* = m_0)(1 - \sum_{n=1,2,...k}(-1)^n(m^*/m_0 - 1)^n)$. By contrast, a linear relationship between effective mass and energy was observed in Ref. [3] for the ground state of ^{3}H and ^{3}He, where the three-body potential is a small perturbation of the Hamiltonian, and the effective mass was estimated as $m^*/m_0 = 1.02$.

The results presented in Fig. 2 illustrate the coupling between the 0_1^+ and 0_2^+ states.

Level anti-crossing occurs when the effective mass approach is applied. We systematically increased the effective mass, commencing from a value of $0.9m_0$. During this increment, we observed an anti-crossing of the ground (blue) and excited levels (red), with dual colors indicating entangled states. The crosses on the graph denote the calculated effective mass values and corresponding experimental energies, signifying the entangled states. Note that the ^{12}C level anti-crossing has been also observed in an oscillator trap in Ref. [47].

The general theory of two-level systems [48] stipulates two parameters that influence anti-crossing. The first parameter, W, describes the strength of the coupling and is derived from the overlap integral of the wave functions taken in uncoupled states. The second parameter, Δ, represents the energy difference between the considered levels in the uncoupled scenario. A strong coupling of two states occurs when the coupling parameter W is large and the energy gap Δ is small, according to the relation [49]

$$2W/\Delta > 1. \tag{10}$$

The limit $2W/\Delta \to 0$ corresponds to the condition for uncoupled states. By using Fig. 2, we can approximate the value of W. The energies of the coupled states are expressed by the following formula [48]

$$E_+, E_- = \frac{1}{2}((E_0 + E_1) \pm \sqrt{(E_0 - E_1)^2 + 4W^2}). \tag{11}$$

Here, E_0 and E_1 denote the energies of the uncoupled ground and first excited states, respectively, with a difference of $\Delta = |E_0 - E_1|$. We have selected the effective mass value corresponding to the condition of $E_0 = E_1$which is the point of intersection of the dot and dashed lines in Fig. 2. In this scenario, the energy difference $E_+ - E_-$ of coupled states can be roughly evaluated as 2 MeV. Utilizing Eq. (11), we have determined $W \sim$2 MeV that is a value comparable to the characteristic energy difference of 7.3/2 MeV. The ratio $2W/\Delta$ serves as an approximation for Eq. (10). Consequently, the coupling between the 0_1^+ and 0_2^+ states can be characterized as weak. Table I outlines the results of the Faddeev calculations for the energy levels of ^{12}C, specifically focusing on the 0_1^+, 0_2^+, and 2_1^+ levels. The 0_1^+ and 2_1^+ levels are identified as bound states, whereas 0_2^+ manifests as a resonance near the three-body threshold. The energy of this resonance is estimated using linear interpolation on an auxiliary parameter, resulting in a bound state below the break-up threshold (see Ref. [22]). Both the effective mass approach and the model incorporating a three-body potential

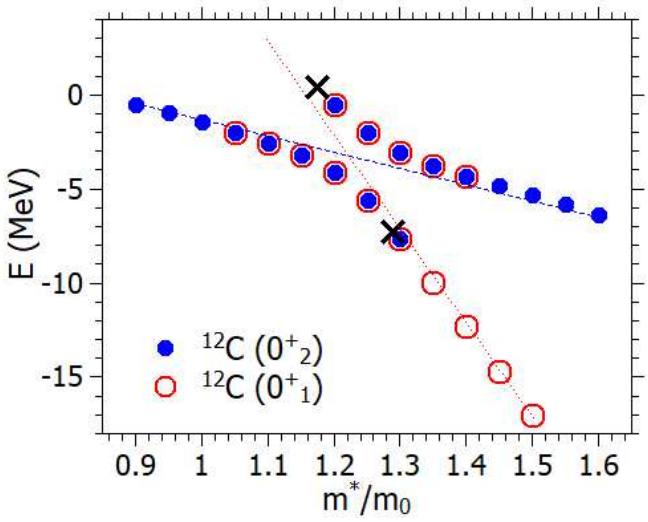

FIG. 2. The level anti-crossing of the first two 0^+ states in ^{12}C within the effective mass approach. The crosses correspond to the α particle effective mass value shown for each state. Dual symbols mark the entanglement states. The dot and dashed lines show the imaginary crossing of the levels according to the linear relation of Eq. (5).

are employed. In the former, the effective mass is fine-tuned to align with the experimental data for the corresponding level. In the latter, the suitable parameters of the three-body potential are determined.

In both approaches, we compute the contributions of the kinetic and potential energy terms of the Hamiltonian (Eq. 1) to the overall energy. These contributions are presented as average values of the corresponding operators, denoted as $\langle E\rangle = \langle H_0\rangle + \langle V_{2bf}\rangle + \langle V_{3bf}\rangle$. Table I also includes a numerical assessment of the MEC effect for the bound states, 0^+_1 and 2^+_1. The scaling parameter α and the effective mass are computed as illustrated in Fig. 1. The asymmetry in scaling with the parameters α and β becomes evident when comparing the values of $\langle H_0\rangle$ and $\langle V_{2bf}\rangle$. The α-scaling amplifies both the kinetic and potential terms.

For each energy level, we identify the three-body potential parameters that exhibit the closest correlation with the effective mass model. The potential in Eq. (9) encompasses two free parameters, strength V and range b, which cannot be solely determined by the energy of the bound state. We leverage the inherent correspondence between an effective mass and the contribution of a three-body potential, assuming that the correction of the particle mass (or the kinetic energy operator) must compensate the contribution of the potential.

We select the parameters of the three-body force to obtain approximate relations where

the matrix element $\langle V_{2bf}\rangle$ and the value of $\langle H_0\rangle + \langle V_{3bf}\rangle$ are similar within both models. This approach provides additional conditions for the parameters of the three-body potential.

The parameters obtained are included in the caption of Tabl. I. The strength of the potential for the ground state is the highest among the states considered. The relative contribution of the three-body potential term is maximal for the 0_1^+ state and decreases subsequently for the 0_2^+ and 2_1^+ levels. Trying to use the three-body potential determined for the ground state to calculate the energy of the 0_2^+ resonance results in a negative value corresponding to a bound state (see the fourth row of the table). It is evident from this table that the matrix

TABLE I. The 3α binding energy and the contributions of kinetic and potential energy terms of the Hamiltonian (1) (in MeV) to the energy E; Eq. (2) is used with the parameters $\beta = 1/m^*$ and α; here, $\langle E\rangle = \beta\langle H_0\rangle + \alpha\langle V_{2bf}\rangle + \langle V_{3bf}\rangle$; the parameters of the three-body potential in Eq. (9) are (a) V = 743.53 MeV, b = 1.253 fm, (b) V = 101.47 MeV, b =1 .9139 fm, (c) V= 288.93 MeV, b=1.3534 fm; the AB potential [8] is used as a pair interaction.

State	Model	m^*/m_0	α	E	$\langle H_0\rangle$	$\langle V_{2bf}\rangle$	$\langle V_{3bf}\rangle$	$\langle E\rangle$
0_1^+	AB+eff.mass	1.292	1	-7.28	56.7	-64.0	–	-7.3
		1	1.2557	-7.28	58.5	-65.8	–	-7.3
	AB+3bf	1	1	-7.28	90.0	-63.1	-34.2[(a)]	-7.3
0_2^+	AB+3bf	1	1	-0.86	40.3	-27.2	-14.0[(a)]	-0.9
	AB+3bf	1	1	–	26.9	-22.4	-4.25[(b)]	0.2
	AB+eff.mass	1.167	1	–	23.0	-22.8	–	0.26
2_1^+	AB+eff.mass	1.148	1	-2.93	41.4	-44.3	–	-2.9
		1	1.1379	-2.93	43.4	-46.3	–	-2.9
	AB+3bf	1	1	-2.93	48.2	-43.6	-7.5[(c)]	-2.9

elements $\langle V_{2bf}\rangle$ of the two-body potential, calculated within both the (AB+ eff.mass) and (AB+3bf) models for the 0_1^+ ground state, exhibit similarity. These results correspond to the first and third rows of Table I. The disparity between them is approximately 1.4%. One can write $\langle V_{2bf}\rangle_{\rm AB+eff.} \approx \langle V_{2bf}\rangle_{\rm AB+3bf}$. One can assume, that the same observation applies to the matrix element of the square of the hyper-radius: $\langle \rho^2\rangle_{\rm AB+eff.mass} \approx \langle \rho^2\rangle_{\rm AB+3bf}$. Further

details on the calculations for root mean square radius and form factors can be found in Ref. [14, 50], where the identical (AB+3bf) model was employed.

For the 0_2^+ resonance, the numerical method developed for the bound state cannot be directly applied. In this case, a method of linear interpolation into the region of positive energy was proposed, motivated by the procedure of analytic continuation in relation to the coupling constant[18, 22, 51]. The resulting interpolation is shown in Fig. 3. The contribution of the kinetic and potential terms corresponding to the Hamiltonian of the 0^+2 state is estimated. For the effective mass model, the calculated values are the matrix elements $\langle E\rangle = \langle H_0\rangle$ and $\langle V2bf\rangle$ for different parameters β, where $\beta = m^*/m_0(1+\zeta)$, and the effective mass is m/m_0=1.167, given the condition $|\zeta| \ll 1$.

We calculate the corresponding matrix elements for a model with a three-body potential for various values of the parameter ζ : $V_{3bf} = V_{3bf}(1+\zeta)$, where the potential V_{3bf} is selected from option (b) in Table I. The average energy is calculated as $\langle E\rangle = \langle H_0\rangle + \langle V_{2bf}\rangle + \langle V_{3bf}\rangle$. The interpolation (solid lines in Fig. 3) was calculated approximating the linear term of the Taylor series, as in Eqs. (4)-(5).

Using the AB potential, the effective mass of the 0_2^+ state of the ^{12}C is evaluated as $1.167m_0$. It is apparent that the effective mass approach could substitute a cluster model with a three-body potential, such that the magnitude of the mass correction compensates for the contribution of the three-body potential. Our study incorporates various models for the α–α interaction to provide a comprehensive analysis. The considered models include the Ali-Bodmer (AB) [8, 14], Yamada-Schuck (YS) [40], and Bhoi-Upadhyay-Laha (BUL) [52] pair potentials. These potentials accurately represent the ^{8}Be(0^+) resonance, which is particularly relevant given the distinct ^{8}Be+α structure of the 0_2^+ state. It is crucial to emphasize that the three-body potential must be a perturbation of the three-body Hamiltonian within the proposed approach. Additionally, the effective mass m^*/m_0 must satisfy the condition within a small vicinity around 1:

$$|1 - m^*/m_0| \ll 1. \tag{12}$$

This constraint is approximately satisfied for the AB potential for both the ground and excited states. However, the BUL potential is relatively weak and fails to form a bound state when $m^*/m_0 = 1$. The AB, YS, and BUL potentials exhibit somewhat different short-distance behaviors, as illustrated in Fig. 4(a). Both AB and BUL potentials depend on the

orbital quantum numbers, $L = 0, 2, 4$, while the effective potential YS only has an s-wave component. The AB potential, in particular, shows strong nuclear repulsion in the s-wave at distances less than 2 fm. Evidently, the specific characteristics of the interactions can influence the calculation results for the effective mass of the 0_2^+ resonance. Nevertheless, the effective-mass approach, when applied with the AB and YS potentials, yields similar effective mass values, approximating around $1.2m_0$. The outcomes of these calculations are depicted in Fig. 4(b).

The BUL potential exhibits less strength than the AB potential. The repulsive core of the BUL potential appears at distances less than 1 fm, and the α–α attraction is shallower than that of the AB potential. The effective mass required to replicate the energy of the ^{12}C bound state is roughly $0.4m_0$, and the energy of the second state 0^+ is reproduced with an effective mass of approximately $0.35m_0$. These values diverge significantly from a perturbative approximation, and the condition (12) is not met. We can thus infer that this

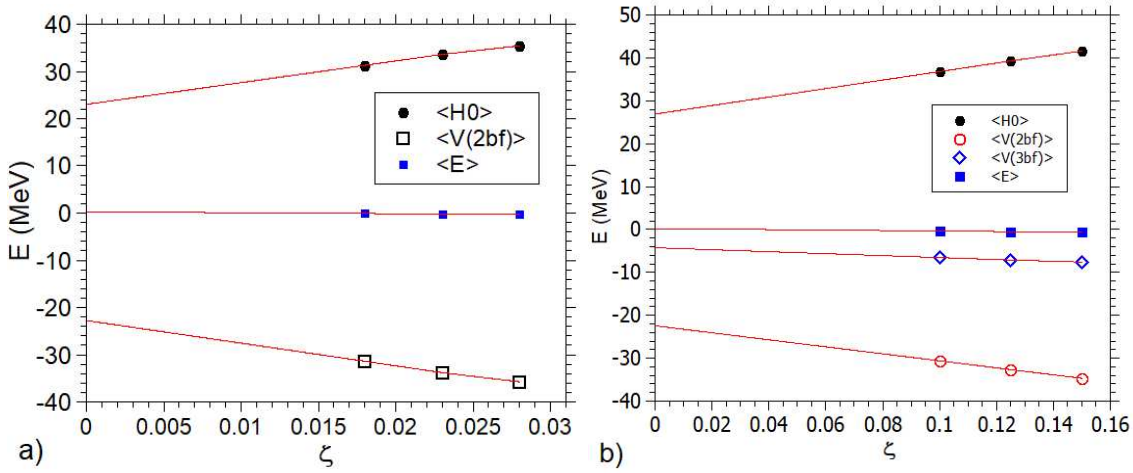

FIG. 3. The kinetic and potential energy contributions for the 0_2^+ bound state. (a) Calculations were carried out for different values of the β parameter, $\beta = m^{/}m_0(1+\zeta)$, where the effective mass $m^{/}m_0$=1.167 and $|\zeta| \ll 1$. (b) Calculations were also performed for different values of the parameter ζ : $V3bf = V_{3bf}(1+\zeta)$, where the potential V_{3bf} is the version (b) from Table I. The solid circles and open squares (rhombus) correspond to the kinetic $\langle H0\rangle$ and potential $\langle V(2bf)\rangle$ ($\langle V(3bf)\rangle$) terms, respectively. The solid squares represent the energy calculated as $\langle E\rangle = \langle H0\rangle + \langle V(2bf)\rangle(+\langle V(3bf)\rangle)$. Interpolation (solid lines) was calculated by approximating the linear term (5) of the Taylor series.

potential is too weak to generate a 0_2^+ state near the breakup threshold.

The YS potential was specifically designed to mimic the molecular state of the 3α system near the three-body threshold. However, this potential results in a weakly bound state for $m^*/m_0 = 1$. To address this, a repulsive three-body potential was introduced in Ref. [40] to adjust the energy of the 0_2^+ resonance to the experimentally observed positive value. Within the effective mass approach, increasing the effective mass is required to achieve a similar energy decrease, as illustrated in Fig. 4(b). This contrasts with the situation for the AB potential. The weakly repulsive nature of the AB potential necessitates an attractive three-body force for the 3α model of the ^{12}C nucleus.

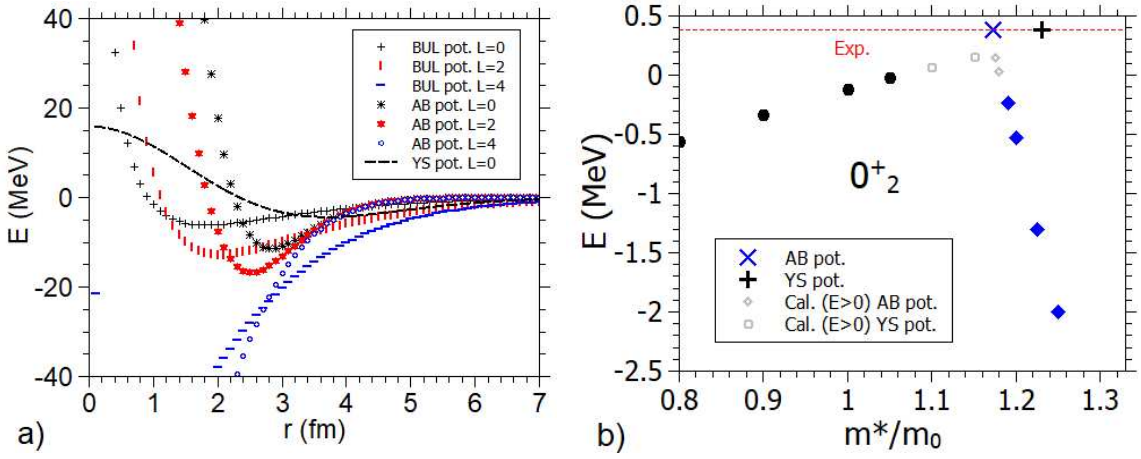

FIG. 4. (a) The Ali–Bodmer (AB) [8, 14], Yamada–Schuck (YS) [40], and Bhoi–Upadhyay–Laha (BUL) [52] α-α potentials. The nuclear components corresponding to the orbital quantum numbers $L = 0, 2, 4$ are differentiated by various symbols. (b) The energy E of the 0_2^+ bound state calculated for different values of the α particle effective mass, m^*/m_0. The solid rhombus and circles correspond to calculations performed using the Ali–Bodmer and Yamada–Schuck α–α potentials, respectively. Calculations above the three-body threshold (marked as "Cal. $(E > 0)$") are indicated by smaller gray symbols. The horizontal dashed line marks the experimental value for the energy of the Hoyle state (denoted as Exp.). Crosses depict the extrapolated positive energy values.

IV. CONCLUSIONS

In this study, we adopted a phenomenological approach to the 3α-cluster model of the ^{12}C nucleus, where a pair interaction describes existing α–α experimental data. The key feature of this model is the incorporation of a three-body potential. Additionally, our approach involves the application of the effective mass method, leveraging the mass–energy compensation effect, to estimate the effective mass of the first (ground state) and second (Hoyle state) 0^+ states, as well as the first 2^+ state. The Faddeev calculations for the bound 3α system demonstrate the mass–energy compensation for a three-body Hamiltonian using the Ali-Bodmer α–α potential. This potential fails to provide the correct value for the ground state of the ^{12}C nucleus without incorporating a three-body potential, which can be fitted to match ^{12}C experimental data. The MEC effect permits the use of an α-particle effective mass as a substitute for the three-body force. This effective mass can variate near the free mass of the α particle and can be phenomenologically estimated by a correspondence to experimental data. The results yield values of approximately $1.292m_0$ for the ground state, about $1.167m_0$ for the Hoyle state, and around $1.148m_0$ for the 2_1^+ state.

We discerned a coupling between the initial two 0^+ states, and this connection can be elucidated through the application of the two-level systems theory [48]. The anti-crossing illustration, constructed on the energy/effective mass plane, serves as compelling evidence of the entanglement between these states. In line with this interpretation, the non-zero coupling matrix elements of this quasi-doublet arise from the overlapping of the wave functions of the involved states.

In our approach, the effective mass is correlated with the strength of the three-body potential, as exemplified in the case of the AB potential. By employing experimental data and scrutinizing the matrix elements of the three-body Hamiltonian terms, two free parameters of the three-body potential can be fine-tuned. We conducted a comparative analysis between the contribution $\langle V_{3bf}\rangle$ of the three-body potential and the averaged kinetic energy terms $\langle H_0\rangle_{3bf\ \mathrm{model}}$ of the cluster model, juxtaposed with the three-body potential and the effective mass model $\langle H_0\rangle_{\mathrm{ef.mass}}$. The relationship

$$\langle H_0\rangle_{\mathrm{ef.mass}} \approx \langle V_{3bf}\rangle + \langle H_0\rangle_{3bf\ \mathrm{model}}$$

establishes an additional criterion (the first being the experimental value of binding energy) for defining the parameters of the three-body potential. The introduction of effective mass

addresses our challenges in describing cluster systems where the traditional notion of a cluster structure is violated at short distances.

We utilized three phenomenological models AB [8], YS [40], and BUL [52] to examine the α–α interaction for evaluating the effective mass in the 0_2^+ state. Our findings reveal that the BUL potential is unsuitable for 3α calculations, failing to produce a bound state and necessitating a robust three-body potential adjustment to achieve the desired energy, thereby compromising the integrity of the cluster model. Conversely, the AB and YS potentials yield comparable effective mass values, approximately $1.2m_0$, despite variations in the energy-mass dependence for each potential. The matrix element $\langle V_{3bf}\rangle$ of the Hamiltonian $H_0+V_{2bf}+V_{3bf}$ can be compensated for by adjusting the effective mass. This adjustment leads to the simplified Hamiltonian H_0+V_{2bf} within the framework of the effective mass approximation. This alteration in mass influences the kinetic energy matrix element $\langle H_0\rangle$, the sign of which is contingent on the sign of $\langle V_{3bf}\rangle$. The attractive or repulsive contribution of the three-body potential determines the dependence of energy on the effective mass, a phenomenon demonstrated in the 0_2^+ state for the AB and YS potentials.

ACKNOWLEDGMENTS

The National Nuclear Security Administration award NA0003979, and the US National Science Foundation, DMR-2101220, DMR-2101041, HRD-1345219 awards, and DHS Award 2016-ST-062-000004 support this work.

---

[1] C. Kittel, *Introduction to Solid State Physics* (8th Edition, Wiley, 2004).

[2] U.G. Meißner, A.M. Rakhimov, A. Wirzba, and U. T. YakhshievEur. Phys. J. A **31**, 357 (2007).

[3] I. Filikhin, V. M. Suslov, B. Vlahovic, Phys. At. Nucl. **86**, 931 (2023); ; arXiv: 2112.13827 [nucl-th].

[4] I. Filikhin, Yu. B. Kuzmichev, B. Vlahovic, Few Body Syst. **65**, 3 (2024).

[5] I. Filikhin, A. Karoui, B. Vlahovic, Int. J. Mod. Phys. E **31**, 2250098 (2022).

[6] J. A. Wheeler, Phys. Rev. **52**, 1083 (1937).

[7] F. Hoyle, Astrophys. J., Suppl. Ser. **1**, 121 (1954).

[8] S. Ali, A. R. Bodmer, Nucl. Phys. **80**, 99 (1966).

[9] B. Buck, H. Friedrich and C. Wheatley, Nucl. Phys. A **275**, 246 (1977).

[10] O. Portilho, D. A. Agrello, S. A. Coon, Phys. Rev. C **27**, 2923 (1983).

[11] H. Kamada H and S. Oryu, Prog. Theor. Phys. **76**, 1260 (1986).

[12] M. Kamimura, Nucl. Phys. A **351**, 456 (1981).

[13] E. Hiyama, M. Kamimura, T. Motoba, T. Yamada, Y. Yamomoto, Progr. Theor. Phys. **97**, 881 (1997).

[14] I. Filikhin, V. M. Suslov and B. Vlahovic, J. Phys. G: Nucl. Part. Phys. **31**, 1207 (2005).

[15] R. Pichter, H. Oberhummer, A. Csoto, and S. A. Moszkowski, Nucl. Phys. A **618**, 55 (1997).

[16] D. V. Fedorov, A. S. Jensen, Phys. Lett. B **389**, 631 (1996).

[17] Y. Fujiwara, K. Miyagawa, M. Kohno, Y. Suzuki, D. Baye, and J.-M. Sparenberg, Phys. Rev. C **70**, 024002 (2004).

[18] N. Tanaka, Y. Suzuki, K. Varga, and R. G. Lovas, Phys. Rev. C **59**, 1391 (1999).

[19] A. Tohsaki, H. Horiuchi, P. Schuck, and G. Ropke, Phys. Rev. Lett. **87**, 192501 (2001).

[20] S. I. Fedotov, O. I. Kartavtzev, V. I. Kochkin, A. V. Malykh, Phys. Rev. C **70**, 014006 (2004).

[21] S. I. Fedotov, O. I. Kartavtsev, A. V. Malykh, Eur. Phys. J. A **26**, 201 (2005) .

[22] C. Kurokawa and K. Kato, Phys. Rev. C **71**, 021301(R) (2005).

[23] C. Kurokawa and K. Kato, Nucl. Phys. A **792**, 87 (2007).

[24] Sh-I. Ohtsubo, Y. Fukushima, M. Kamimura, and E. Hiyama, Prog. Theor. Exp. Phys. **2013**, 073D02 (2013).

[25] Y. Fujiwara and R. Tamagaki, Prog. Theor. Phys. **56**, 1503 (1976).

[26] O. Portilho, S. A. Coon, Z. Physik A **290**, 93 (1979).

[27] S. Ishikawa, J. Phys.: Conf. Ser. **312**, 042010 (2011).

[28] T. Suhara, Y. Kanada-En'yo, Phys. Rev. C **91**, 024315 (2015).

[29] M. Freer, H. Horiuchi, Y. Kanada-En'yo, D. Lee and Ulf-G. Meißner, Rev. Mod. Phys. **90**, 035004 (2018).

[30] B. Zhou, Y. Funaki, H. Horiuchi, A. Tohsaki Front. Phys. **15**, 14401 (2020).

[31] E.M. Tursunov, I. Mazumdar, Phys. At. Nucl. **85**, 160 (2022).

[32] R. Alvarez-Rodriguez, A. S. Jensen, E. Garrido, D. V. Fedorov, and H. O. U. Fynbo, Phys. Rev. C **77**, 064305 (2008).

[33] R. Alvarez-Rodriguez et al. J. Phys. G: Nucl. Part. Phys. **35**, 014010 (2008).

[34] I. Filikhin, Phys. At. Nucl. **63**, 1527 (2000).

[35] D. V. Fedorov, E. Garrido, A. S. Jensen, Few-Body Syst. **33**, 153 (2003).

[36] R. Alvarez-Rodriguez, A. S. Jensen, D. V. Fedorov, H. O. U. Fynbo, E. Garrido, Europ. Phys. J. A **31**, 303 (2007).

[37] R. Alvarez-Rodriguez, A. S. Jensen, E. Garrido, D. V. Fedorov, H. O. U. Fynbo, Phys. Rev. C **77**, 064305 (2008).

[38] A. A. Ogloblin, A. S. Demyanova, A. N. Danilov, S. V. Dmitriev, T. L. Belyaeva, S. A. Goncharov, V. A. Maslov, W. Trzaska, and S. V. Khlebnikov, EPJ Web Conf. **66**, 02074 (2014).

[39] S. I. Fedotov, O. I. Kartavtsev, A. V. Malykh, Pisma Zh. Eksp. Teor. Fiz. **92**, 715 (2010).

[40] T. Yamada, P. Schuck, Phys. Rev. C **69**, 024309 (2004).

[41] A. Tohsaki, H. Horiuchi, P. Schuck, and G. Ropke, Rev. Mod. Phys. **89**, 011002 (2017).

[42] I. Filikhin, V. M. Suslov and B. Vlahovic, Fiz. B (Zagreb) **20**, 189 (2011).

[43] I. Filikhin, A. Gal, V. M. Suslov, Nucl. Phys. A **743**, 194 (2004).

[44] S. P. Merkuriev, L. D. Faddeev, *Quantum Scattering Theory for Several Particle Systems* (Kluwer Academic, Dordrecht, 1993).

[45] R. Machleidt, Few-Body Syst. **64**, 77 (2023).

[46] J. L. Friar, B. F. Gibson and G. L. Payne, Phys. Rev. C **42**, 1211 (1990).

[47] D.V. Fedorov, A.S. Jensen, M. Thogersen, Few-Body Syst. **45**, 191 (2009).

[48] C. Cohen-Tannoudji, B. Diu, F. Laloe, *Quantum Mechanics*, Vol. 1 (Wiley VCH, 1992).

[49] I. Filikhin, A. Karoui, T. Zatezalo, S.P. Kruchinin, and B. Vlahovic, Mod. Phys. Lett. B **38**, 2342005 (2023); DOI: 10.1142/S0217984923420058.

[50] I. Filikhin and S. Yakovlev, Phys. At. Nucl. **63**, 343 (2000).

[51] V. I. Kukulin, V. M. Krasnopolsky, and J. Horachek, *Theory of Resonances: Principles and Applications* (Kluwer Academic, Dordrecht, Netherlands, 1989) p. 219.

[52] J. Bhoi, R. Upadhyay, and U. Laha, Commun. Theor. Phys. **69**, 203 (2018).